

1. Motivation

- ❖ Multi-frequency radar measurements can improve retrieval of snowfall properties from satellite observations
- ❖ Dual-Frequency Ratio (DFR): Reflectivity difference between two radars operating at different frequencies
- ❖ DFR is related to characteristic size D_m , used to retrieve particle size distribution (PSD) parameters, and influenced by microphysical processes

Research Questions

1. What can multi-frequency radar measurements tell us about the microphysics in snowstorms?
2. How are these observations related to banded precipitation structures?

2. Data & Methods

- ❖ W-band (CRS), Ku- and Ka-band (HIWRAP), X-band (EXRAD) reflectivity Z_e corrected for attenuation and matched to P-3 location
- ❖ PSDs: 2D-S (0.15–1.4 mm, 10 μ m resolution), HVPS (1.4–30 mm, 150 μ m resolution) every 5 s
- ❖ Scattering simulations from Leinonen & Szyrmer (2015; LS15) aided in deriving bulk microphysical properties (Fig. 1)

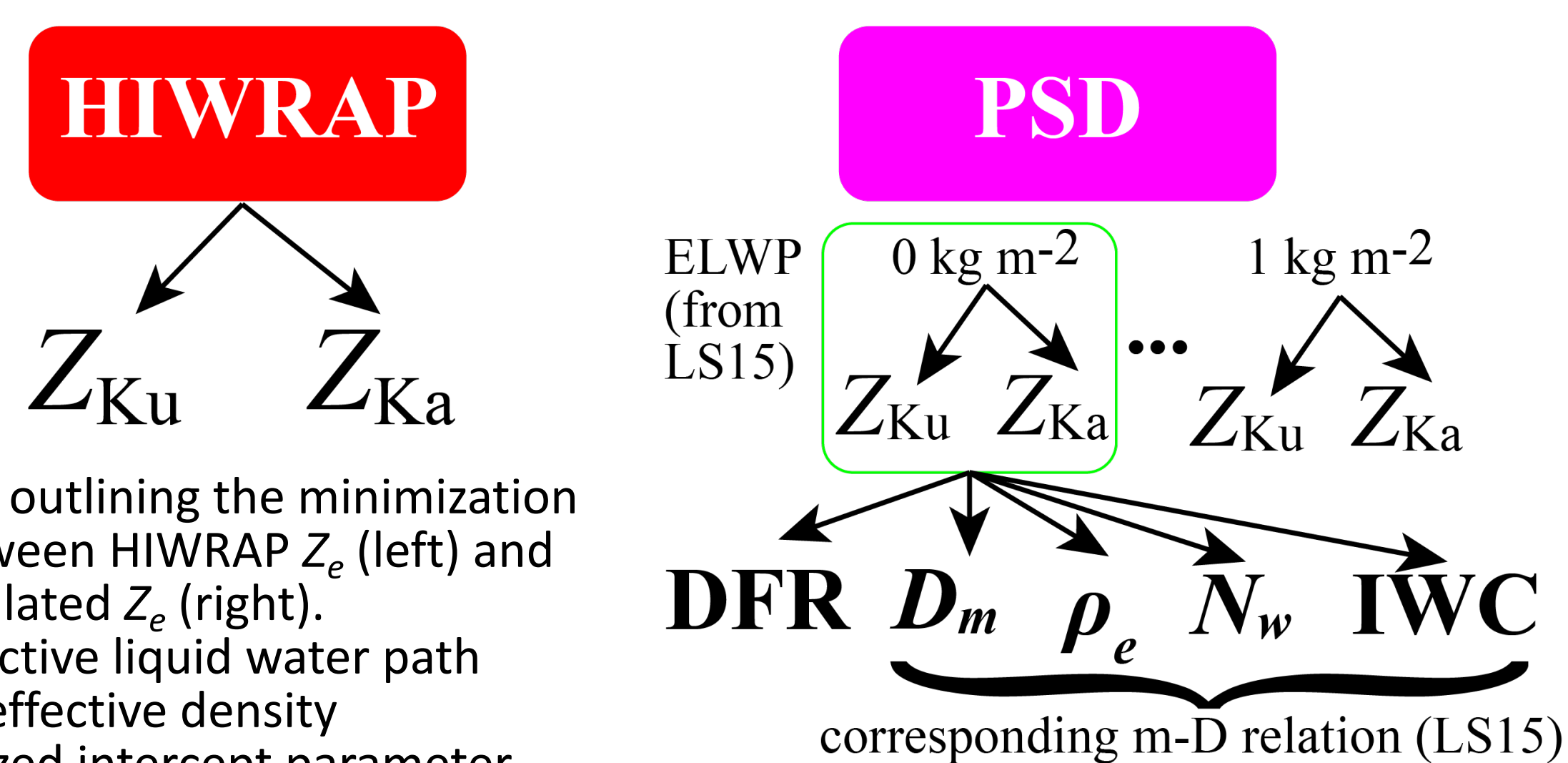


Fig. 1 Schematic outlining the minimization procedure between HIWRAP Z_e (left) and simulated Z_e (right). ELWP = effective liquid water path, ρ_e = effective density, N_w = normalized intercept parameter, IWC = ice water content

- ❖ Variable DFR threshold considering the prominence and relative width of DFR peaks used to investigate whether DFR related to precipitation structures (Fig. 2)

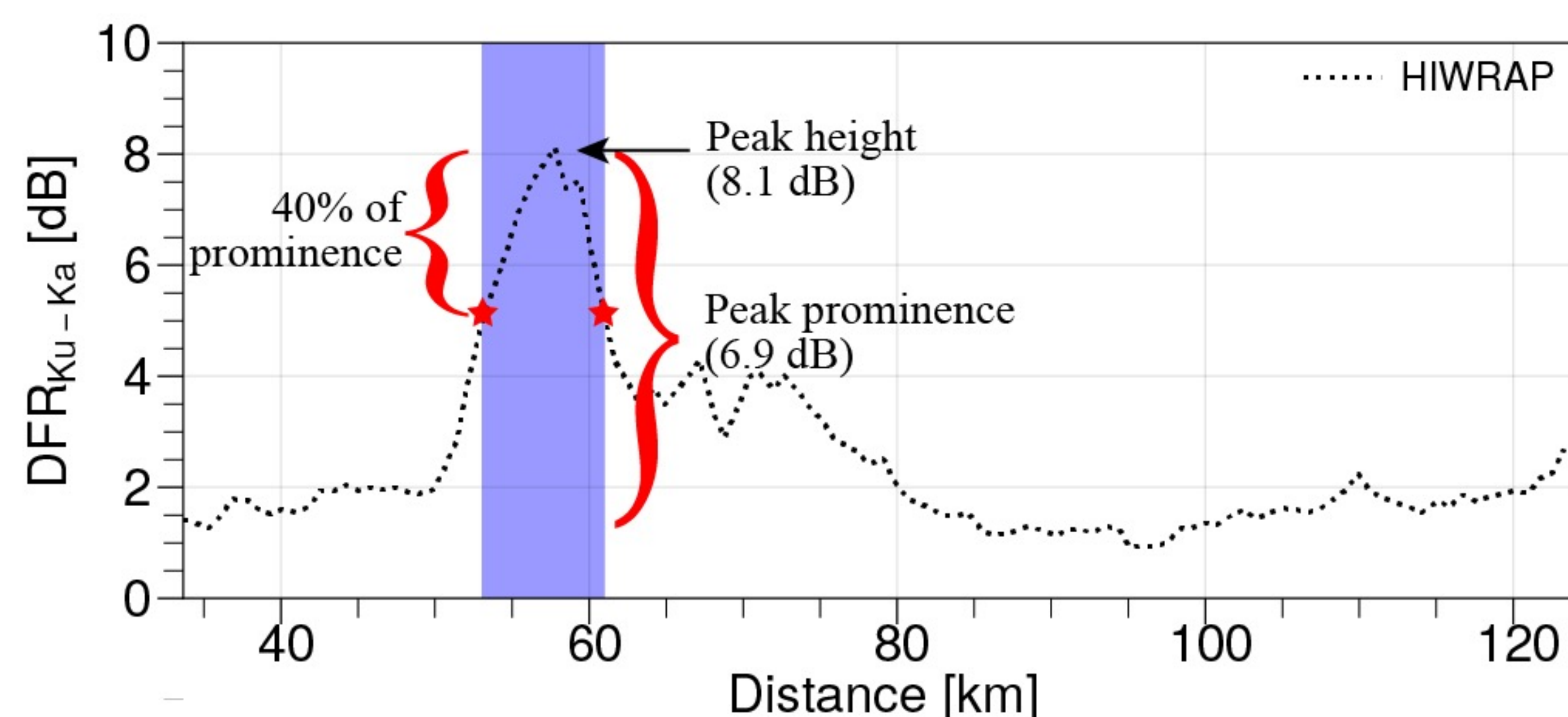


Fig. 2 Example of procedure used to detect prominently larger radar Ku- and Ka-band DFR (DFR_{Ku-Ka}) along the P-3 flight track. All DFR peaks with prominence ≥ 2 dB first identified, with times corresponding to DFR $\geq 40\%$ of the prominence considered a region of enhanced DFR.

3. Regions of Enhanced DFR at Flight Level

Example: 05 February 2020

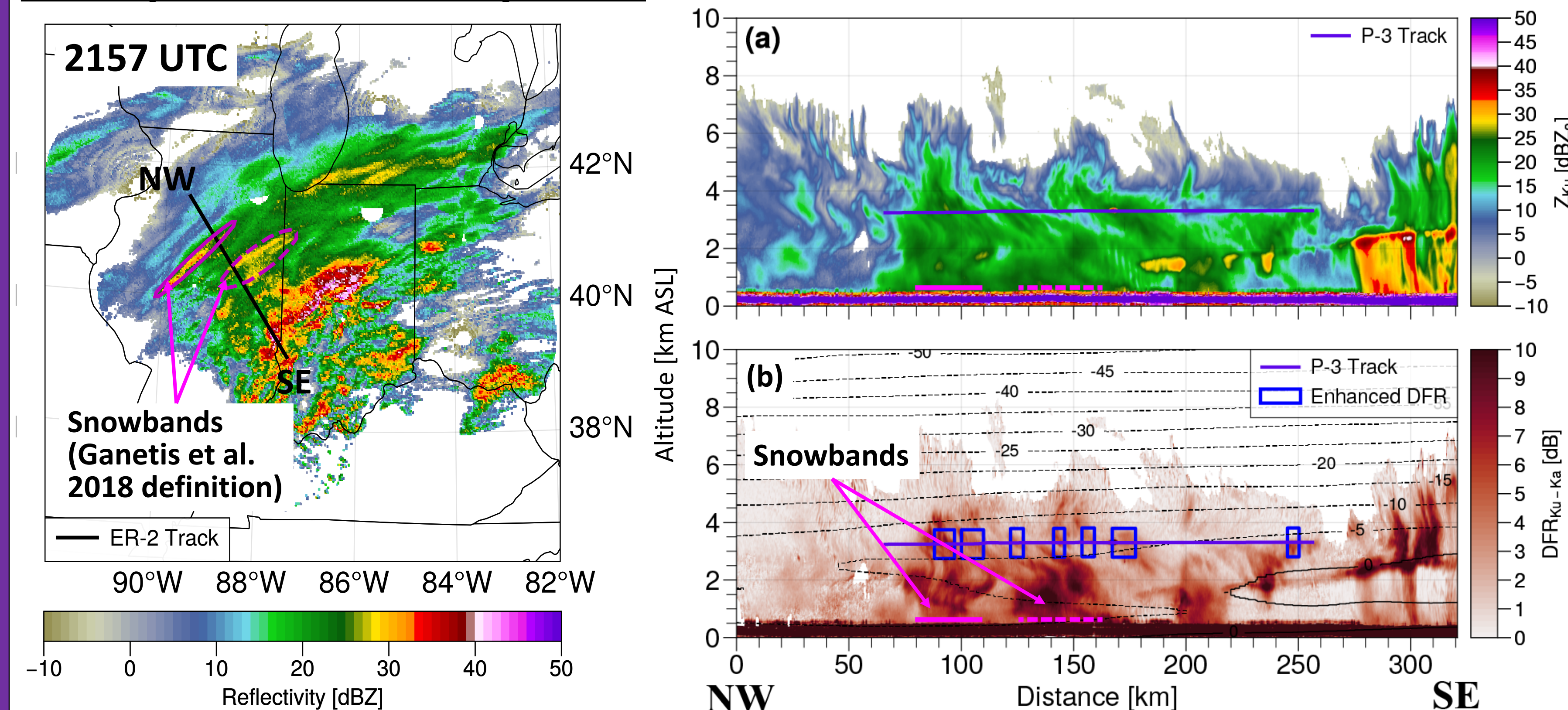


Fig. 3 2-km Z_e from NEXRAD mosaic.

Fig. 4 HIWRAP cross-sections of (a) Z_{Ku} and (b) DFR_{Ku-Ka} . P-3 flight track (purple line) and regions of enhanced DFR (blue boxes).

- ❖ ER-2 and P-3 sampled banded precipitation structures (Figs. 3, 4)
- ❖ Larger D_m , smaller effective density ρ_e and intercept parameter N_w within regions of enhanced DFR consistent with an enhanced aggregation process (Figs. 5, 6)
- ❖ IWC has smaller response to changes in DFR due to having smaller N_w and less dense particles in regions of enhanced DFR

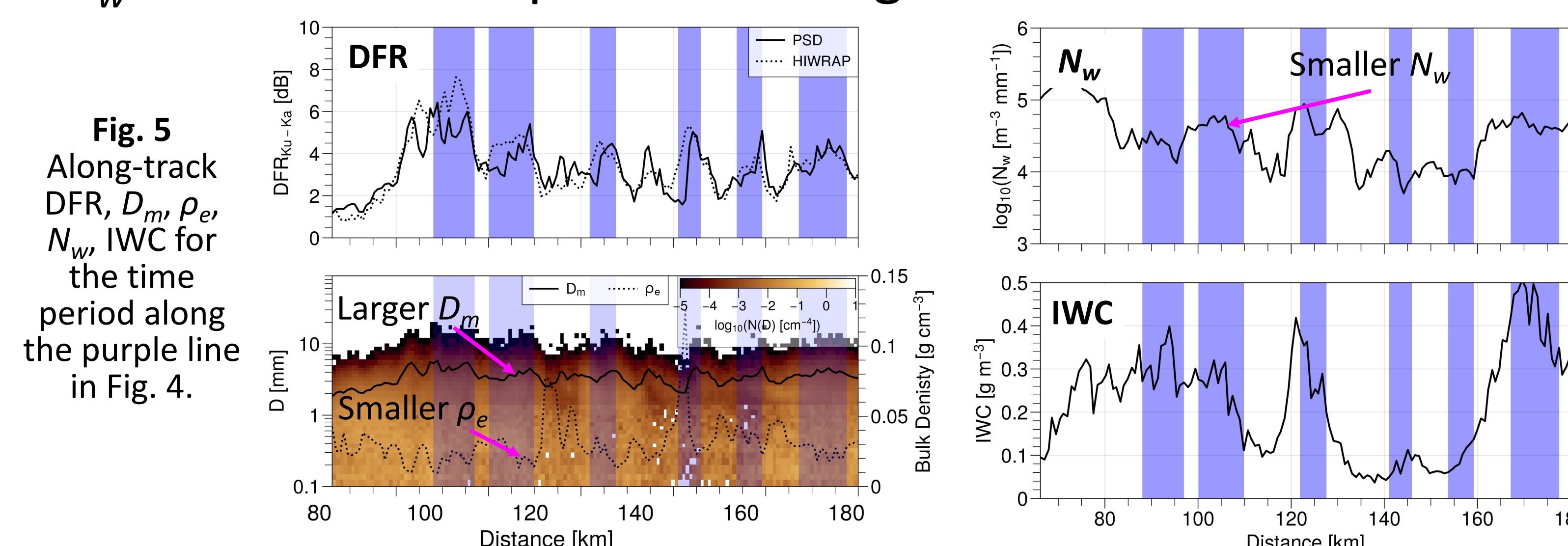


Fig. 5 Along-track DFR, D_m , ρ_e , N_w , IWC for the time period along the purple line in Fig. 4.

All Coordinated Flights

- Enhanced DFR Regions**
- ❖ Larger D_m (+58%)
 - ❖ Smaller ρ_e (-37%)
 - ❖ Smaller N_w (-74%)
 - ❖ IWC values not notably different (-0.9%)

Note: 25 Jan & 01 Feb flights sampled different environments compared to the other flights.

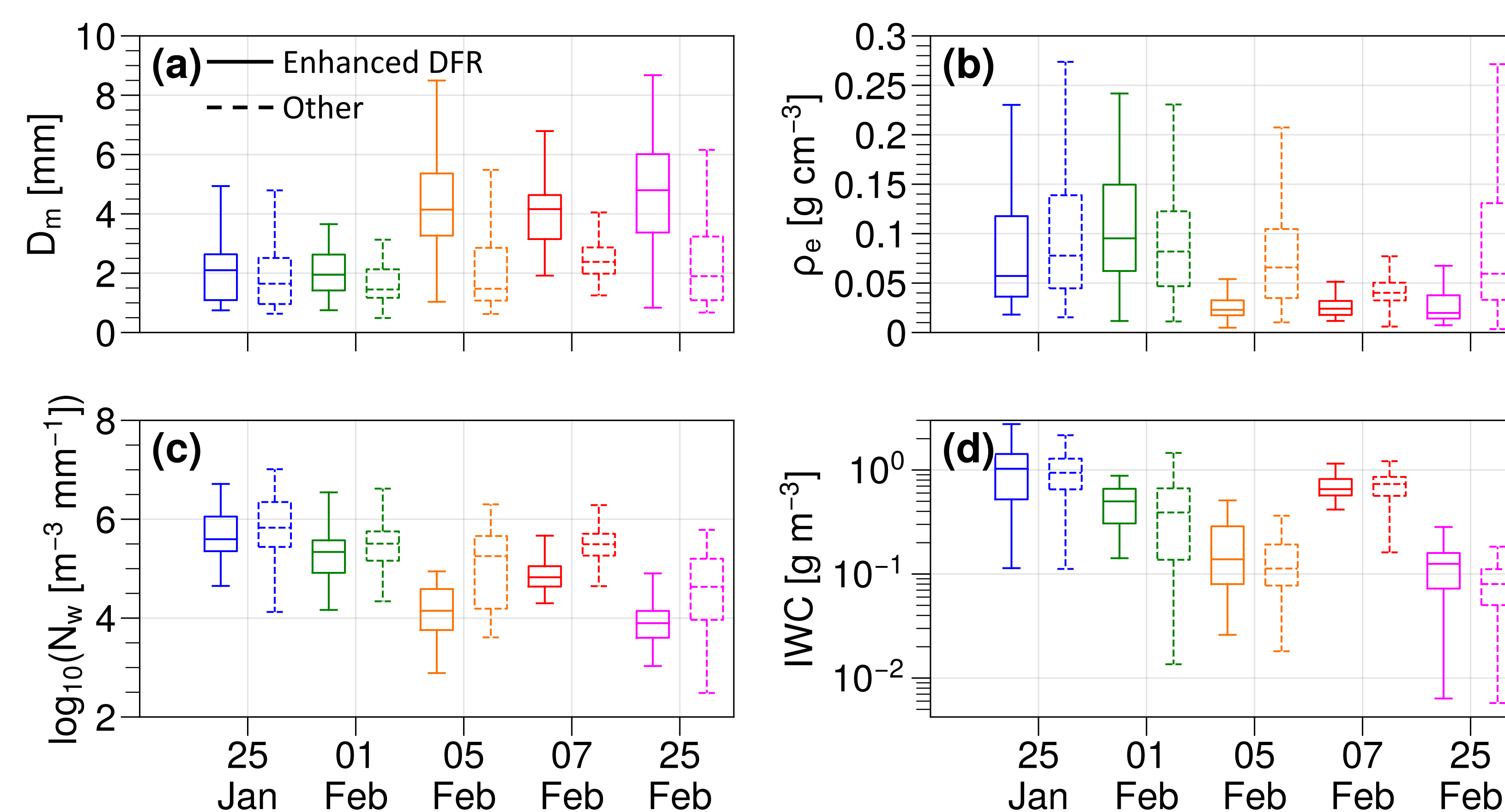


Fig. 6 Boxplots of (a) D_m , (b) ρ_e , (c) $\log_{10}(N_w)$, and (d) IWC for regions within (solid) and outside of (dashed) enhanced DFR for each coordinated flight.

4. Multi-Frequency Results

- ❖ Larger D_m farther from origin of DFR plane and larger ρ_e at lower DFR_{Ku-Ka} consistent with scattering models and past studies
- ❖ "Hook" signature (Fig. 7a) not as pronounced as dendrite and unrimed aggregate models or some past studies (e.g., OLYMPEX)

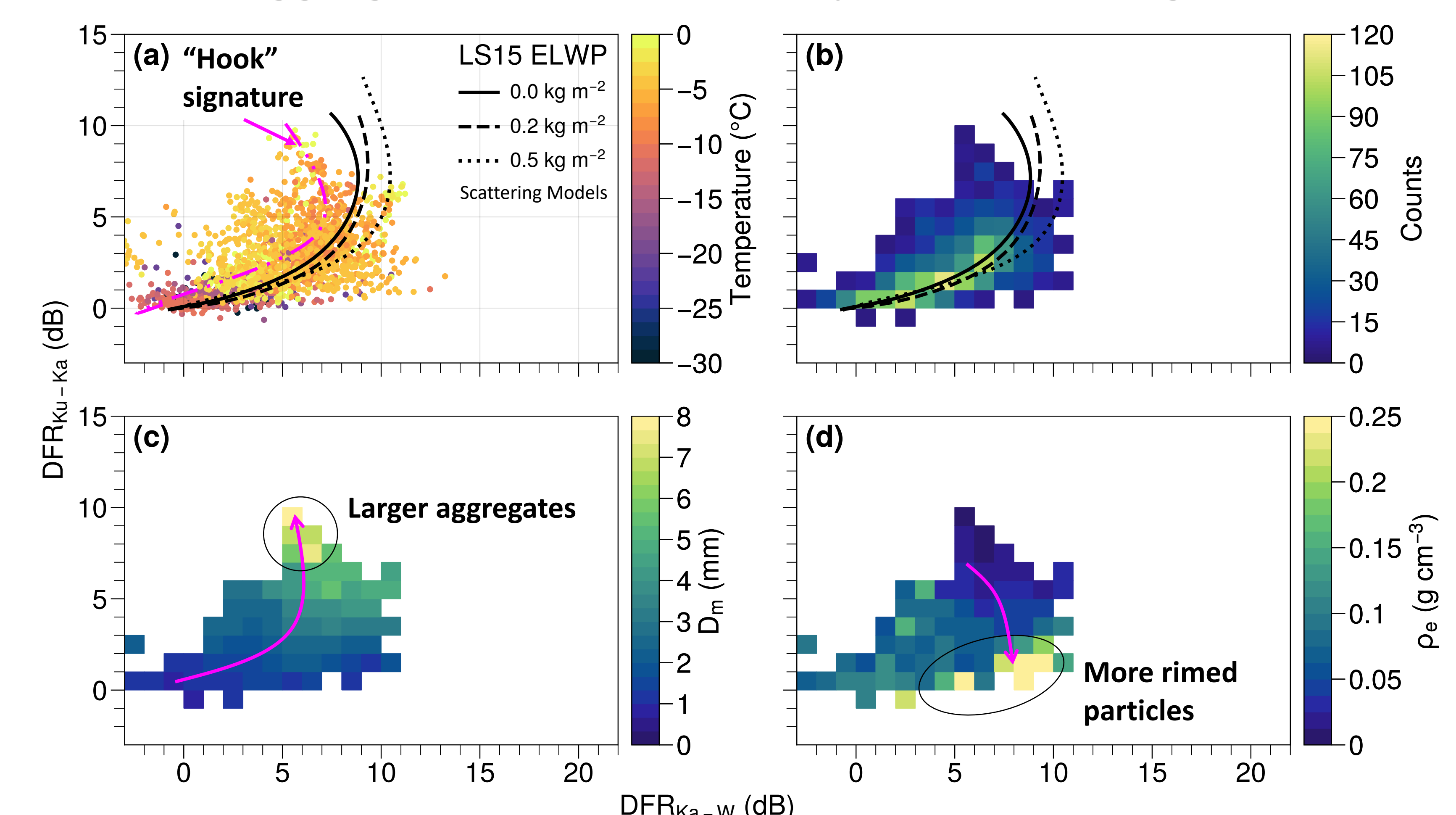


Fig. 7 (a) Scatterplot of temperature as a function of radar DFR_{Ku-Ka} and DFR_{Ka-W} with scattering curves from LS15. Panels (b)–(d): 2D histograms of (b) observation count, (c) mean D_m , (d) mean ρ_e .

5. Retrieved Microphysical Properties

- ❖ Neural network (NN) radar retrieval (Chase et al. 2021) used
- ❖ Negative correlation between D_m and N_w (aggregation; Fig. 8)
- ❖ D_m , N_w , IWC well correlated between NN and observations

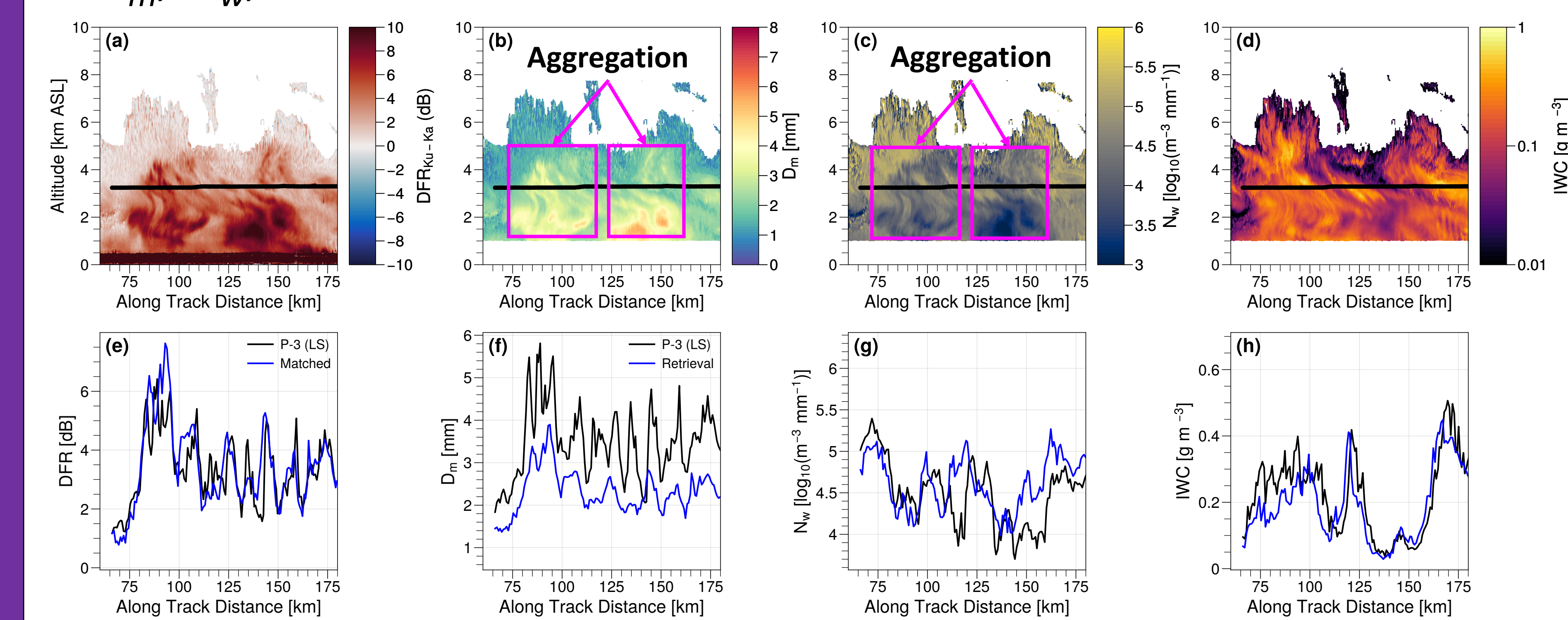


Fig. 8 Top row: Cross-sections of (a) DFR_{Ku-Ka} and retrieved (b) D_m , (c) N_w , and (d) IWC for the same flight leg in Fig. 4. Bottom row: Comparison of the same properties as in (a-d) between the P-3 observations and the NN.

6. Conclusions

- ❖ Enhanced DFR associated with aggregation and co-located with regions identified as snowbands by Ganetis et al. (2018) criteria
- ❖ Neural network radar retrievals of microphysical properties compares well with observations
- ❖ Ultimately, NN based on DFR may be used to develop retrievals of microphysical properties from space-borne measurements

References

- ❖ Leinonen and Szyrmer, 2015: Radar signatures of snowflake riming: A modeling study. DOI:10.1002/2015EA000102.
- ❖ Chase et al., 2021: A Dual-Frequency Radar Retrieval of Two Parameters of the Snowfall Particle Size Distribution Using a Neural Network. DOI: 10.1175/JAMC-D-20-0177.1.
- ❖ Data publicly available at the NASA GHRC, DOI: 10.5067/IMPACTS/DATA101
- ❖ This work is funded by the NASA grant 80NSSC19K0338

Contact

Joseph Finlon
jfinlon@uw.edu
<https://github.com/joefinlon>

